Journal of Engineering Physics and Thermophysics, Vol. 80, No. 4, 2007

ANALYSIS OF MASS-TRANSFER PHENOMENA IN THE DENDRITIC NET OF SOLIDIFYING STEEL INGOTS. 2. CONVECTIVE DIFFUSION OF THE IMPURITY IN THE DENDRITIC NET OF SOLIDIFYING INGOTS

Ya. A. Samoilovich,[a] **V. I. Timoshpol'skii,**[b] **and S. M. Kabishov**[c]

UDC 621.746

An analysis of the interaction of the melt flow with the surface of dendritic crystallites has been performed using the concept of a diffusion boundary layer, and the regularities of the impurity distribution over the cross section of ingots and castings in the process of their solidification have been revealed.

During the process of crystallization of steel there is continuous enrichment of the melt with soluble impurities (sulfur, phosphorus) and with certain components of the alloy (carbon, manganese, and others). This process is a consequence of the separation diffusion of the impurities at the crystallization front due to the different degrees of solubility of the elements in the solid and liquid phases. The separation diffusion of soluble impurities leads to the fact that a concentration of the impurity C_{sol} lower than the initial concentration C_0 is established on the surface of crystallites growing in the melt, whereas the melt layer adjacent to the crystallization front becomes enriched with a soluble impurity. In consideration of the process indicated within one crystallite (dendrite), the regularities of the element distribution in the liquid and solid phases have led us to a completed theory of dendritic liquation [1–4].

In the simplest case of the absence of diffusion in the solid phase the relation between the concentration of the impurity on the crystallite surface C_0 and the volume fraction of the solid phase φ is expressed by the Scheil equation [5]

$$C_{sol} = kC_0 (1 - \varphi)^{k_0 - 1} . \tag{1}$$

For γ-Fe-based austenitic steel the coefficient k varies within 0.35–0.36, whereas for δ-Fe (with a carbon content of less than 0.5%) it varies within 0.14–0.20. Figure 1 gives as an example the relation C_{sol}/C_0 as a function of the volume fraction of the solid phase (φ) in accordance with the Scheil equation. It has been proposed in [6] that the "effective distribution coefficient"

$$k_{ef} = \frac{C_{sol}}{C_{liq}} = \frac{k}{k + (1 - k) \exp\left(-\dfrac{v_{cr}\delta}{D}\right)} \tag{2}$$

be used for calculation of the relation of the concentrations in the solid and liquid phases in the movement of the crystallization front with a certain constant velocity v_{cr}.

Attempts at describing theoretically the process of formation of the chemical inhomogeneity in a solidifying ingot (process of macrosegregation) have thus far fallen short of the degree of completeness characteristic of dendritic-liquation theory. The notion of a two-phase zone as the interlacing of dendritic crystallites with the liquid phase in between is widely used in the modern theory of ingot crystallization. At the same time, the substantial influence of the

[a]"Platan" Science and Production Enterprise, Ekaterinburg, Russia; [b]Presidium of the National Academy of Sciences of Belarus, 66 Nezavisimost' Ave., Minsk, 220072, Belarus; [c]Belarusian National Technical University, 65 Nezavisimost' Ave., Minsk, 220013, Belarus. Translated from Inzhenerno-Fizicheskii Zhurnal, Vol. 80, No. 4, pp. 8–12, July–August, 2007. Original article submitted June 19, 2006.

 1062-0125/07/8004-0644

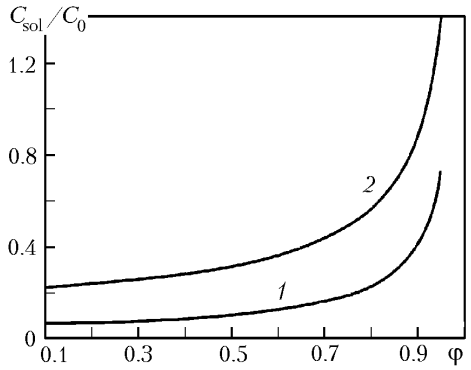

Fig. 1. Concentration of carbon in the solid phase (on the surface of dendritic crystallites) vs. amount of the solid phase in accordance with the Scheil equation: 1) k = 0.14 and C = 0.40; 2) 0.353 and 0.57.

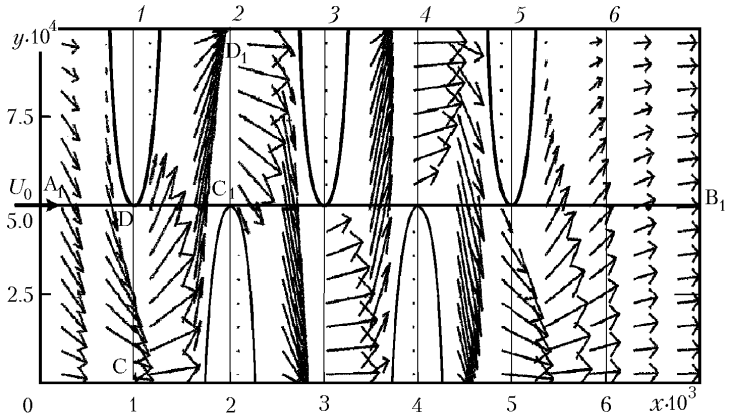

Fig. 2. Pattern of melt flows between dendrite branches and layout of control cross sections: 1–4) two-phase zone; 5) boundary of the two-phase zone; 6) liquid phase. y and x, m.

motion of a melt in the unsolidified part of an ingot and particularly within the two-phase zone on the impurity distribution over the cross section of the ingot is accepted.

In [7–9], in describing the interaction of the two-phase zone of an ingot with its liquid core, use has been made of the motion of a diffusion boundary layer arranged at the boundary running along the vertices of dendritic crystallites that formed the two-phase zone. In the present work, the concept of a diffusion boundary layer is used in analyzing the interaction of the melt flow with the surface of dendritic crystallites.

The process of propagation of a soluble impurity in the two-phase zone of a solidifying ingot is investigated by solution of the coupled system of differential equations

$$\frac{\partial C}{\partial t} + \nabla (C\mathbf{U}) = \nabla (D\nabla C) , \tag{3}$$

$$\rho \frac{\partial \mathbf{U}}{\partial t} - \mu \nabla^2 \mathbf{U} + \nabla p = \mathbf{F} . \tag{4}$$

Integration of Eqs. (3) and (4) is carried out in the computational element ABCD (see Fig. 1 in [10] and Fig. 2), including five secondary branches of two neighboring dendritic crystalites. The results of solution of the Navier–Stokes equation (4) in describing the melt motion in the interdendritic space have been presented in [10]. Let us turn our at-

tention to an analysis of mass-exchange phenomena accompanying the interaction of the melt flow with the surface of dendritic branches.

We assume that the process of transfer of a substance from the surface of dendritic branches proceeds by the following mechanism:

(a) the separation diffusion of the impurity occurs in the boundary layer, with the result that the concentration of the impurity on the solid-phase surface is $C_{sol} < C_0$, and in the boundary layer, it is $C_b > C_0$;

(b) the involvement of the excess amount of the impurity from the boundary layer in the main flow of the melt proceeds by the convective mechanism and is characterized by the mass-transfer coefficient β dependent on the flow velocity and the physical properties of the melt [11].

Under such assumptions, at the boundary of the melt flow and the surface of dendritic branches, the boundary condition

$$-D\frac{\partial C}{\partial n} = \beta\,(C_b - C) \tag{5}$$

holds true. In addition to condition (5), the convective-diffusion equation (3) is accompanied by the following boundary conditions:

(a) for $x = 0$ (along the AB line of the computational element ABCD), we have

$$C = C_0\,; \tag{6}$$

(b) at $t = t_0$, we have

$$C = C_0\,. \tag{7}$$

In numerical integration of Eq. (3), we use the running values of the components of the vector of melt-flow velocities **U** (they have been determined in [10]). The intensity of involvement of the impurity from the surface of dendritic crystallites in the melt flow is allowed for by the mass-transfer coefficient β computed in terms of the Sherwood number Sh from the criterial equation [11, p. 494]

$$\mathrm{Sh} = 0.33\mathrm{Re}^{0.5}\mathrm{Sc}^{0.33}\,, \tag{8}$$

where $\mathrm{Sh} = \beta L/D$, $\mathrm{Re} = \rho w L/\mu$, and $\mathrm{Sc} = \mu/\rho D$.

Taking the values of the physical parameters $\rho = 7000$ kg/m^3, $\mu = 0.0062$ Pa·sec, and $D = 10^{-8}$ m^2/sec for austenitic steel, we obtain a relation between the Sherwood number and the Reynolds number: $\mathrm{Sh} \cong 1.47\mathrm{Re}^{0.5}$. On prescription of the above physical characteristics of the steel melt and $L = 10^{-3}$ m, we find the dependence of the mass-transfer coefficient on the flow velocity in the form $\beta = 0.494 \cdot 10^{-3} w^{0.5}$ m/sec.

Considerations applied to selection of the parameters β and C_b in boundary condition (5) complete the formulation of the problem of convective diffusion of the impurity in the computational element ABCD of the dendritic net of a solidifying steel ingot.

Numerical integration of Eqs. (3) and (4) has been performed by the finite-element method with the subdivision of the computational domain ABCD into a fairly large number of elements (more than 1200), which ensured high-accuracy computations. A description of the hydrodynamic situation in the interdendritic space of element ABCD has been presented in [10] where certain features of melt flow past the secondary branches of dendritic crystallites have been noted. The results of numerical solution of the convective-diffusion equation (3) with account for boundary conditions (5)–(7) are given in Figs. 3 and 4.

It is noteworthy that the nonstationary character of the solution of this problem manifests itself as the presence of the initial "acceleration" stage whose duration is 10–12 sec for the selected dimensions of the computational element and the physical properties of the melt; thereafter the concentrations of the impurity at all points of the computational element attain certain stationary values for the instant of time $t = 20$ sec.

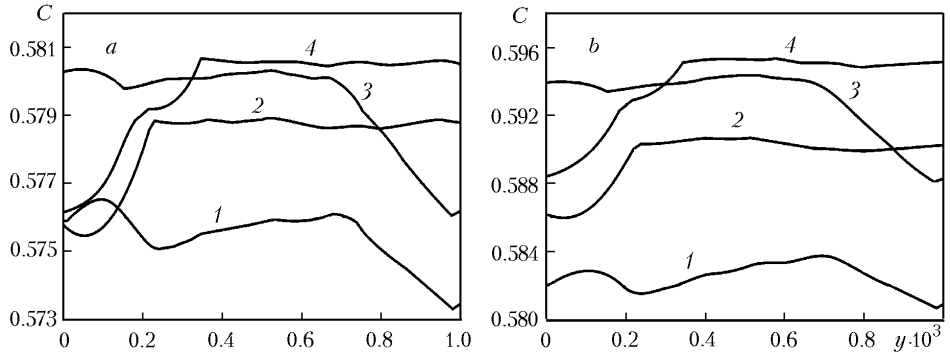

Fig. 3. Carbon distribution along the vertical cross sections 1–4 for the prescribed C_0 = 0.57% and U_0 = 0.1 mm/sec: a) C_b = 0.75 and b) 1.0%. C, %; y, m.

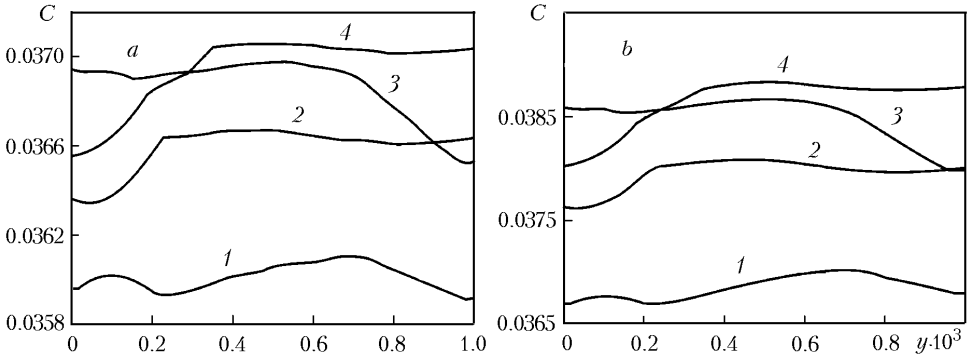

Fig. 4. Sulfur distribution along the vertical cross sections 1–4 for the prescribed C_0 = 0.035% and U_0 = 0.1 mm/sec: a) C_b = 0.07 and b) 0.1%. C, %; y, m.

We have investigated the distribution of the concentrations of carbon and sulfur over the cross section of the computational element; the initial values of the concentrations were taken to be C_0(C) = 0.57% and C_0(S) = 0.035%. It is precisely such values that were recorded in experimental steel ingots of mass 50 kg and diameter 240 mm in [12] where the formation of macroliquation in solidifying steel has been studied.

The results (presented in Figs. 3 and 4) of a computational analysis point to the fact that the concentrations of iron and sulfur in the moving melt gradually grow, as it moves in the interdendritic space. For quantitative evaluation of the degree of the above growth, we successively recorded the element concentrations obtained by calculation in cross sections 1, 2, 3, and 4 (see Fig. 2).

An analysis of the plots enables us to draw the following conclusions.

1. The accumulation of carbon in the melt flow from cross section to cross section is observed; the absorption of the element is maximum in the first step (between cross sections 1 and 2), whereas on the next portions (from 2 to 3 and from 3 to 4), the increases in the carbon concentration are gradually reduced.

2. The impurity distribution over the height of control cross sections reflects somewhat the pattern of melt flow past secondary branches. Indeed, cross sections 2 and 4 are characterized by the presence of two vertical zones (along the coordinate y): in the first zone, we observe a growth in the carbon concentration for y = 0–0.3 mm, whereas in the second zone, for y = 0.3–1 mm, the carbon concentration is maintained constant, in practice, and equal to 0.5788% for cross section 2 and to 0.5805% for cross section 4. We note that the zones of the cross sections for which the concentration of carbon is elevated are open for the melt flow from the previous section of the computational element with a maximum amount of the impurity accumulated due to the mass transfer from the dendrite branch that is located in this section.

Analogous features of the impurity (sulfur) distribution over the height of the control cross sections can be seen in the plots of Fig. 4 which have been obtained for the prescribed C_0(S) = 0.035% and C_b = 0.07% and 0.1%.

TABLE 1. Increase in the Concentration of a Soluble Impurity

Element	C_0, %	C_b, %	Cross sections		
			$1 \rightarrow 2$	$2 \rightarrow 3$	$3 \rightarrow 4$
Carbon	0.57	0.75	0.0028	0.0015	0.0003
		1.0	0.0068	0.0036	0.0008
Sulfur	0.035	0.07	0.00055	0.00021	0.00012
		0.1	0.00110	0.00065	0.00015

The values of the increases in the concentration of a soluble impurity (carbon, sulfur) on different portions of the interdendritic space are given in Table 1.

The average growth in the concentrations of carbon and sulfur in motion of the melt in the computational element of the dendritic net amounts to 0.01% and 0.001% respectively. According to the procedure presented, we have carried out a series of calculations during which the velocity of melt flow (within 0.1–1 mm/sec), the initial concentration of carbon and sulfur, the length of secondary dendritic-crystallite branches, and the length of the computational element were varied. The calculation results enable us to infer that the growth in the concentration of carbon in the melt flow can attain 0.06–0.08% for an average flow velocity of 0.1 mm/sec and a melt-flow path length of 4–5 cm. As a result the concentration of the impurity in the flow attains 0.63–0.65% for an initial concentration of 0.57%. For the sake of comparison we note that a carbon concentration of 0.8–0.9% was recorded in the axial zone of the test steel ingots [12]. Thus, the fraction of the growth in the amount of the impurity due to the transfer in the melt flow for this case is no higher than 20–25%. Needless to say, the evaluation performed is quite arbitrary, since we disregarded a possible reduction in the permeability of the dendritic net along the flow path length and the change in the indices of dispersity of the dendritic net. Nonetheless, it may be stated that the "translational" component of the growth in the concentration of soluble elements in a solidifying ingot due to the involvement of the impurity in the moving melt can make up a substantial share of the growth in the concentration of the elements in the axial zone of solidifying steel ingots.

NOTATION

C, concentration of the impurity in the melt, %; C_0, initial concentration of the impurity in the melt, %; C_{liq} and C_{sol}, concentration of the impurity in the liquid and solid phases, %; C_b, concentration of the impurity in the boundary layer, %; D, diffusion coefficient of the impurity in the liquid phase, m^2/sec; **F**, external-force vector; k, distribution coefficient of the impurity; k_{ef}, effective distribution coefficient of the impurity; L, characteristic dimension of the flow, m; n, normal to the surface; p, pressure, Pa; Re, Reynolds number; Sc, Schmidt number; Sh, Sherwood number; **U**, velocity vector; t, time, sec; v_{cr}, crystallization-front velocity, m/sec; w, melt velocity, m/sec; y, coordinate axis; β, mass-transfer coefficient, m/sec; δ, thickness of the diffusion boundary layer, m; μ, dynamic viscosity of the melt, Pa·sec; ∇, Hamiltonian operator; ρ, density, kg/m^3. Subscripts: 0, initial; cr, crystallization; ef, effective; liq, liquid; b, boundary; sol, solid.

REFERENCES

1. I. N. Golikov, *Dendritic Segregation in Steel* [in Russian], Metallurgizdat, Moscow (1958).
2. I. I. Novikov and V. S. Zolotorevskii, *Dendritic Segregation in Alloys* [in Russian], Nauka, Moscow (1966).
3. V. A. Efimov, *Casting and Crystallization of Steel* [in Russian], Metallurgiya, Moscow (1976).
4. M. C. Flemings, *Solidification Processes* [Russian translation], Mir, Moscow (1977).
5. E. Scheil, Beitrag zum Problem der Blockseigerung, *Zeit. Metallkunde*, **34**, 70–75 (1942).
6. J. A. Burton, R. C. Prim, and W. P. Slichter, *J. Chem. Phys.*, **21**, 1987–1991 (1953).
7. F. Oeters and M. Seidler, *Archiv f.d. Eisenhuttenwessen*, **48**, No. 9, 481–486 (1974).
8. F. Oeters and Z. Zhong, Principles of macrosegregation caused by mixing flow in the bulk melt, *Steel Res.*, **56**, No. 3, 137–146 (1985).

9. Z. Zhong, H. Dorr, and F. Oeters, Theoretical and experimental investigation on macrosegregation caused by mixing in the liquid bulk melt, *Steel Res.*, **56**, No. 6, 306–312 (1985).
10. Yu. A. Samoilovich, V. I. Timoshpol'skii, and S. M. Kabishov, Analysis of mass-transfer phenomena in the dendrite net of solidifying steel ingots. 1. Formulation of the problem. Analysis of melt flow in the dendritic net, *Inzh.-Fiz. Zh.*, **80**, No. 4, 3–7 (2007).
11. C. O. Bennet and J. E. Myers, *Momentum*, *Heat, and Mass Transfer* [Russian translation], Nedra, Moscow (1996).
12. L. Huang and K. Schverdtfeger, Onset of macrosegregation in continuous casting of billets, *Chernye Metally*, No. 3, 19–23 (1981).